Superheated Ice: True Compression Fractures and Fast Internal Melting

Abstract. *Internal melt figures can be nucleated in ice without the presence of a vapor bubble. Their form and growth are fracture-like, different from the normal Tyndall stars, which do contain vapor bubbles. Normal Tyndall figures that grow rapidly are not oriented in the basal plane, and very rapid internal melting gives a peculiar, systematic growth of clouds of Tyndall figures.*

Kamb (*1*) stated that it is not possible to nucleate internal melting in ice without the presence of a vapor bubble unless the temperature is substantially above 0°C. The reason is that without a vapor bubble, the negative pressure produced by melting the ice internally could raise the melting point to as high as +8°C. This is, of course, dependent on the strength of the ice. We attempted a simple experiment to produce rapid internal melting and see whether melt figures could nucleate and grow without vapor bubbles.

We produced rapid internal melting by irradiating the ice with a Colortran 1000-watt quartz-iodine lamp in a reflector housing. Rectangular, single-crystal plates of ice, measuring approximately 1 by 3 by 5 cm, were supported at the mouth of the reflector, 4 cm from the bulb. The ice crystals were grown by freezing distilled water in a bucket. In all cases the ice plates were left at room temperature for 5 minutes after their outer surfaces had started to melt, to insure that they were at 0°C throughout. Photographs were taken of the internal melting at intervals of somewhat less than 1 second, by using shadow photography (*2*).

It is easy, with such a setup, to produce internal melting without vapor bubbles. The melt figures are very thin and are curved but oriented roughly in the basal plane of the parent ice crystal; they look exactly like internal, conchoidal fractures. They grow much faster than the normal Tyndall stars, which have vapor bubbles, that often form along with the fractures. Figure 1, a and b, shows the formation of these internal fractures.

These are undoubtedly compression fractures in the true sense of the term. The material on either side of the fracture moves toward the fracture plane. While the ice-water interfaces that are the fracture walls move apart in fracturing, the material of the two walls ends up closer together after fracturing than it was to start with, because of the volume decrease. Although it is difficult to visualize at first, this is the result to be expected from a confined source of negative pressure. We know of no previously reported example of this type of fracturing, although it seems possible that it could occur within the earth. Käss and Magun (*3*) did observe this type of internal fracturing in ice, but attributed it to thermal shock, which our observations show to be incorrect.

The only difference between the internal fracturing and the ordinary internal melting is the absence of a vapor bubble in the fracture. When a vapor bubble nucleates along with the liquid phase, substantial negative pressures can not build up because the liquid can evaporate rapidly into the bubble to fill the extra volume provided by the melting.

As a nucleation problem, the formation of ordinary Tyndall figures is much more complicated than that of internal fractures. Either liquid or vapor may form first, or both may form simultaneously. We may speculate that vapor forms first, with most of the energy barrier having been surmounted at preexisting vacancy clusters. Thus, the first step in the formation of Tyndall figures may be internal evaporation, with melt-

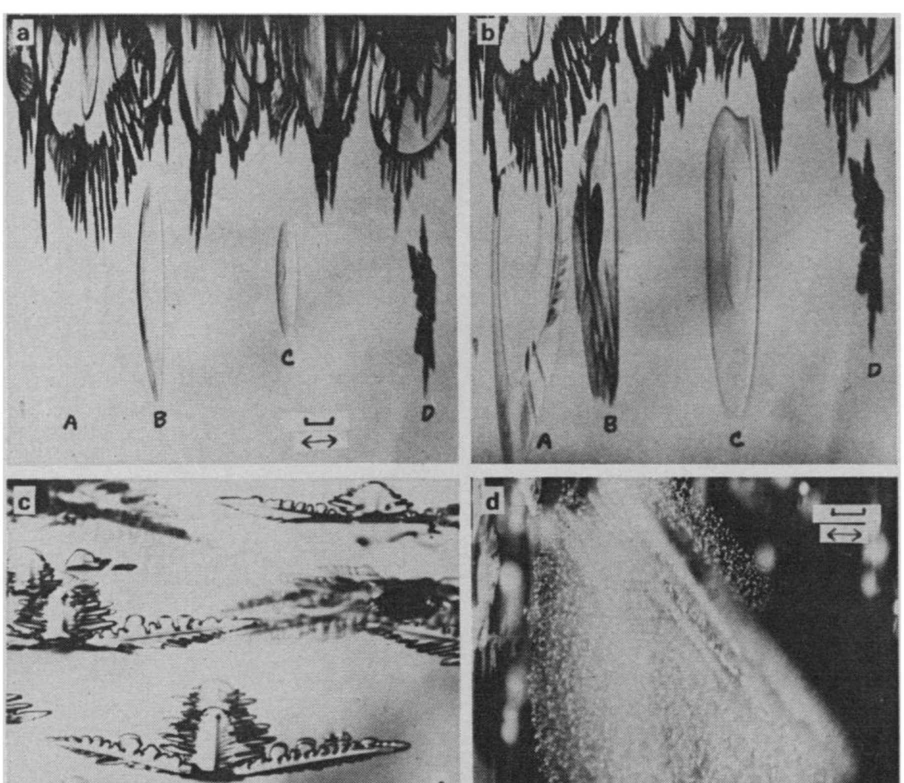

Fig. 1. (a and b) Internal melting without vapor bubbles (*A*, *B*, and *C*) and with a vapor bubble (*D*—the bubble is not visible here). Photographs (a) and (b) were taken ½ second apart. (c) Normal, nonbasal Tyndall flowers, with vapor bubbles. (d) The peculiar, cloudlike growth at very high radiation intensity. The scale marks are 1 mm; the double arrows show the trace of the *c*-axis.

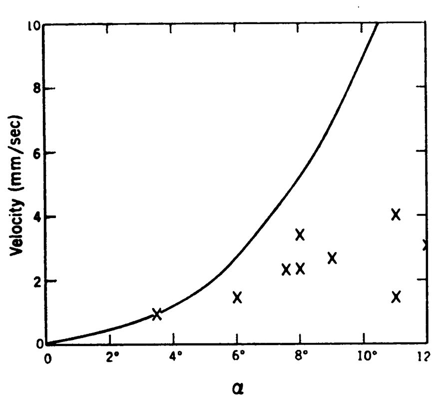

Fig. 2. The line shows the relation between the dendritic growth velocity of ice in supercooled water and the orientation deviation angle α between the dendrites and the basal plane (*4*). The crosses represent corresponding measurements, with melting velocity replacing growth velocity, for internal melting with vapor bubbles. The size of the crosses shows the approximate measurement error for the melting velocity; errors in angle measurement may be as great as 2°.

ing coming later at the ice-vapor interface. The internal pressure needs only to be reduced below the vapor pressure of the ice, by the superheating, for this to become possible.

Another, entirely different kind of internal melting occurs at the highest radiation intensity. Clouds of Tyndall figures grow systematically, often in planes (Fig. 1d). These clouds extend at a rate of roughly 1.5 to 2 cm/sec. The clouds consist of myriads of tiny, hexagonal water pockets, each with its own vapor bubble. Microscopic examination immediately after formation discloses no connecting channels between the pockets. The reason for the systematic growth of these clouds of Tyndall figures must lie in some sort of mechanical linkage—an effect of stress on the nucleation of new melting centers with vapor bubbles—but the details are obscure. This cloudy growth has been described before (*3*) and was explained in the same general way.

An aspect of internal melting that apparently has not been studied is the orientation of the regular melt figures (those with vapor bubbles, not the fractures). Internal melting should be analogous to ice crystal growth in supercooled water. The dendrite orientations of ice grown in supercooled water are well known to change continuously as a function of supercooling, as Pruppacher (*4*) has studied thoroughly. The melt figures, when produced rapidly, should also show variation of dendrite orientation, and, in fact, they do (Fig. 1c).

The only way to compare Pruppacher's data on ice growth with data on internal melting is to compare graphs of the growth and melting velocities plotted against the deviation angle (deviation from basal orientation) (Fig. 2). It is interesting, and puzzling, that there is almost no coincidence here. The value of the angle of deviation at a certain melting velocity is always higher than that at the same freezing velocity, and the melting data are very scattered. It may be possible to attribute this to the fact that the heating is caused by radiation, which is directional. If there is a large, direct heating effect at the ice-water interface, then the melting conditions can be very asymmetric, and the larger, and scattered, values for the deviation angle in melting may be understood.

CHARLES A. KNIGHT
NANCY C. KNIGHT
National Center for Atmospheric Research, Boulder, Colorado 80302

References and Notes

1. B. Kamb, *Science* **169**, 1343 (1970).
2. U. Nakaya, *U.S. Army Snow Ice and Permafrost Res. Estab. Res. Pap. 13* (1956), p. 3.
3. M. Käss and S. Magun, *Z. Kristallogr.* **116**, 354 (1961).
4. H. R. Pruppacher, *J. Chem. Phys.* **47**, 1807 (1967); *J. Glaciol.* **6**, 651 (1967).
5. The National Center for Atmospheric Research is sponsored by the National Science Foundation.

3 May 1972; revised 16 June 1972

Molecular Structure of LSD

Abstract. *The molecular configuration of lysergic acid diethylamide (LSD) in crystals of the iodobenzoate has been determined by using x-ray diffraction techniques. The configuration shows strain and steric hindrance and the conformation is fixed. Some of the implications of this for the hallucinogenic activity of LSD are discussed.*

The molecular understanding of the biological activity of any substance requires a knowledge of its three-dimensional structure. We report here the single crystal structure analysis of lysergic acid diethylamide (LSD) *o*-iodobenzoate monohydrate and briefly discuss some implications of the results.

The crystals are monoclinic, space group $P2_1$, with unit cell parameters $a = 1421(2)$, $b = 765(1)$, $c = 1324(2)$ pm, and $\beta = 115.53(5)°$; the number

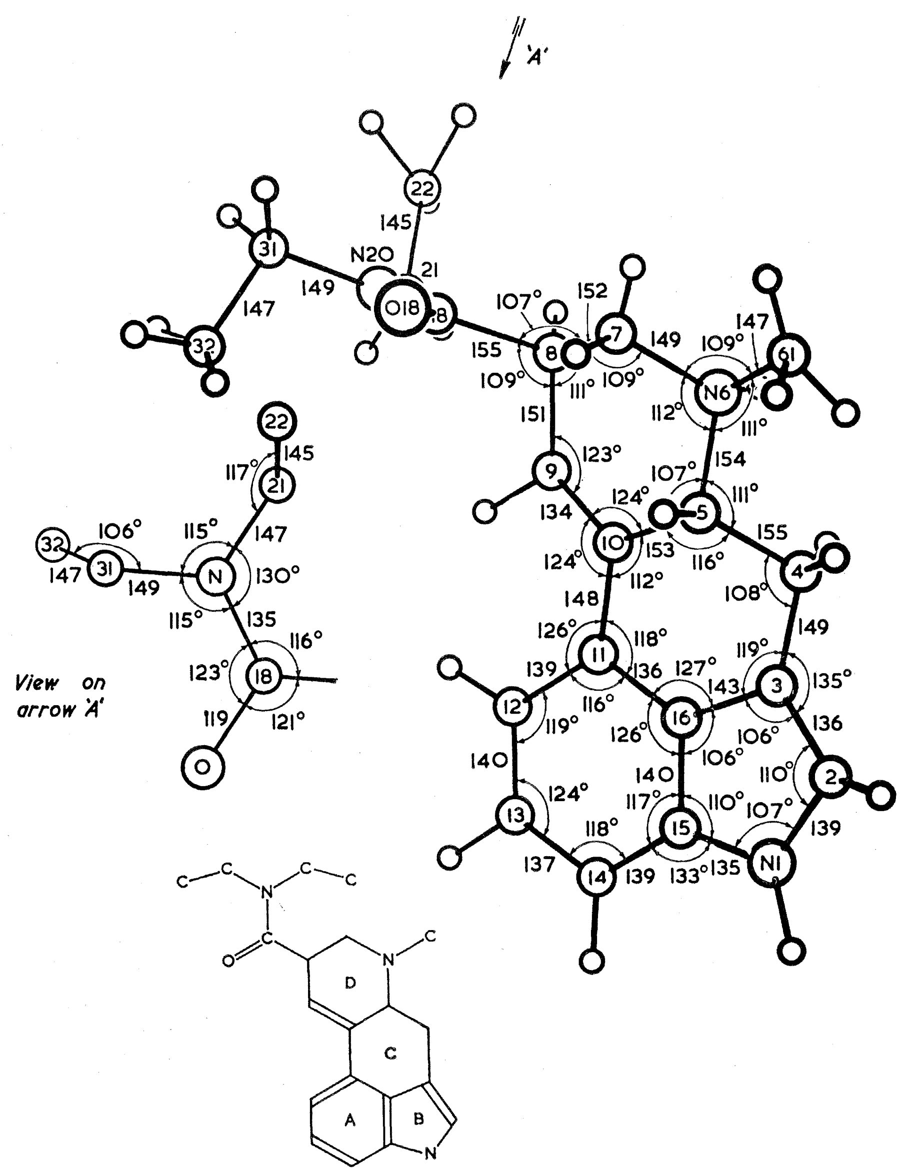

Fig. 1. The observed conformation of the LSD molecule projected onto (010). All the hydrogen positions were found experimentally. The distances and bond angles have standard deviations of 2 pm and 1°, respectively.